

Electronic structure of a mixed valence system: Eu_3O_4

B. Batlogg, E. Kaldis, A. Schlegel, and P. Wachter

Laboratorium für Festkörperphysik, Eidgenössische Technische Hochschule Zürich, 8049 Zürich, Switzerland

(Received 23 June 1975)

The optical reflectivity of single crystals of Eu_3O_4 has been investigated in the photon energy range between 0.03 and 12 eV. The dielectric functions have been derived by means of a Kramers-Kronig analysis and interpreted with lattice vibrations and interband transitions from initial Eu^{2+} , Eu^{3+} , and $2p^6$ states into crystal-field-split $5d$ bands. In addition intra $4f^6$ transitions have been observed and commented on. The Coulomb correlation energy between Eu^{2+} and Eu^{3+} has been found experimentally. Optical transmission measurements at low temperatures have revealed a blue shift of the absorption edge for temperatures above the Néel point T_N and in zero external magnetic fields and a red shift of the absorption edge for magnetic fields larger than a critical field $H_c = 2.4$ kOe, confirming the metamagnetic phase. T_N is found to be 5.2 ± 0.2 K.

I. INTRODUCTION

Mixed valence systems are compounds where the cation is present in more than one valence state. Some well known examples are Fe_3O_4 (magnetite),¹ Eu_3S_4 ,² and Sm_3S_4 ,³ the chemical formula of which can be written $A^{2+}A_2^{3+}B_4^{2-}$. If the cations occupy equivalent lattice sites, then a temperature activated hopping process occurs between the divalent and the trivalent cation, and at high temperatures Mössbauer measurements yield an intermediate valence of the cation of 2.5.⁴ This is the case in the above-mentioned materials. Magnetite crystallizes in the inverse spinel structure with eight Fe^{3+} and eight Fe^{2+} ions occupying octahedral B sites and eight Fe^{3+} ions being in tetrahedral A sites and Eu_3S_4 and Sm_3S_4 crystallize in the Th_3P_4 structure, where all cation sites are equivalent. The latter two materials are of further interest since at low temperatures a charge-ordering effect has been proposed⁵ and possibly been observed in the case of Eu_3S_4 .²

On the other hand, Eu_3O_4 ($\text{Eu}^{2+}\text{Eu}_2^{3+}\text{O}_4^{2-}$) is a compound with divalent and trivalent Eu being in the ratio 1:2, but the Eu ions occupy nonequivalent lattice sites, since this material crystallizes in the calcium ferrite (CaFe_2O_4) structure.⁶ Here divalent Eu occupies the Ca sites and trivalent Eu the Fe sites. The trivalent Eu ions are coordinated to six oxygen ions forming distorted octahedra, and the divalent Eu ions are coordinated to eight oxygen ions, six of which form a triangular prism with the Eu in the center, and two oxygen ions are located out from the two wide faces of the prism.⁶ Therefore, hopping mobility and intermediate valence are not expected in this material. On the other hand, if the electronic structure of Eu_3O_4 were known, it might serve as a reference structure for Eu_3S_4 or Sm_3S_4 , and absorbing regions in the latter two compounds not being accounted for by similar absorptions in Eu_3O_4 may then be connected with the hopping mechanism.

With regard to the magnetic properties of

a Néel temperature quoted between 5 and 7.8 K and with a critical field of $H_c = 2.4$ kOe.⁷⁻⁹ In this connection, it is of considerable interest to investigate the influence of magnetic order on the optical spectra.

II. SYNTHESIS OF MATERIAL

Eu_3O_4 was synthesized by reacting EuO and Eu_2O_3 in stoichiometric ratio (7-g charge) in an evacuated and sealed molybdenum crucible. Details about the sealing process by electron bombardment and the apparatus and furnaces used can be found elsewhere.¹⁰ In order to avoid changes in stoichiometry due to partial evaporation of the most volatile components, the reaction of the starting materials and the crystal growth of Eu_3O_4 were made in a reverse transport temperature profile, keeping the lid of the crucible hotter than the bottom. The crucible was heated for 30 h at 1900°C ($\Delta T = -40^\circ\text{C} = 1860-1900^\circ\text{C}$), then for 5 h at 2040°C ($\Delta T = -50^\circ\text{C} = 1990-2040^\circ\text{C}$) and then cooled slowly ($10^\circ\text{C}/\text{h}$). Crystals with dimensions $3 \times 3 \times 2$ mm were obtained. A small part of the starting materials of EuO and Eu_2O_3 did not react and was found at the surface of the melt which solidified last. The nonreacted components were easily distinguished by their different color with respect to Eu_3O_4 . X-ray powder diagrams gave lattice constants similar to those of the literature^{6,11}: $a = 10.095$, $b = 12.070$, and $c = 3.501$ Å.

III. REFLECTIVITY AND KRAMERS-KRONIG ANALYSIS

The reflectivity of mechanically polished and annealed single crystals of Eu_3O_4 has been measured at room temperature for photon energies between 0.03 and 12 eV. The results are shown in Fig. 1 with the insert giving a blown up view of the far-infrared data. The general pattern of the reflectivity is that of an insulator with ionic vibrations in the infrared and electronic interband transitions in the visible and ultraviolet. Insulating behavior is expected from the chemical formula and the crys-

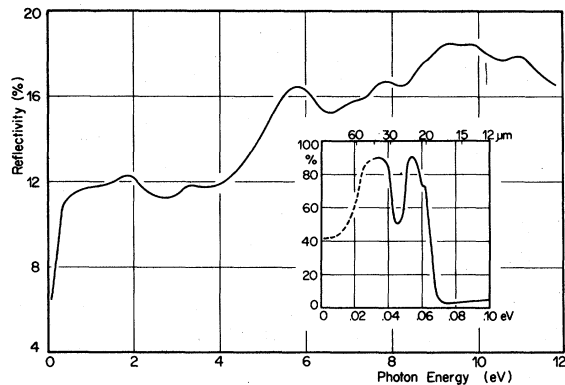


FIG. 1. Reflectivity of Eu_3O_4 single crystals at 300 K. The insert shows the reflectivity in the far infrared. Dashed part of the curve is extrapolated as described in the text.

tallographic structure and has also been verified with a four-probe resistivity measurement at 300 K, yielding $\rho \geq 10^6 \Omega \text{ cm}$. For photon energies below 0.08 eV, the reflectivity is due to the residual rays. Compared with EuO ,¹²⁻¹⁴ it is remarkable that the minimum in the reflectivity (3%) due to the LO phonon modes is with 0.073 eV (17 μm) at higher energies in Eu_3O_4 and that after a shoulder and a maximum at 0.0515 eV (24 μm), we observe a second minimum at 0.045 eV (27.5 μm) and a maximum near 0.031 eV (40 μm). Considering the detailed structure analysis of Rau,⁶ we realize that the phonon modes can be substituted by two TO modes and two LO modes, in spite of the fact that a group-theoretical analysis of the complex structure will result in many more modes. However, the latter superimpose in a reflectivity experiment and cannot be distinguished individually. The double-phonon structure basically arises due to the different oxygen surrounding of trivalent and divalent Eu. In the Eu^{3+} oxygen octahedrons, the Eu-O distance is always less (with an average of 2.34 \AA) than the one in EuO (2.57 \AA), and in the Eu^{2+} oxygen prisms the Eu-O distance is always more (with an average of 2.71 \AA) than the one in EuO . Consequently, we have hard TO and LO modes due to the Eu^{3+} surrounding and softer TO and LO modes due to the Eu^{2+} surrounding.

The lowest photon energy used has been 0.03 eV (40 μm). For this energy we observe already a small decrease of the reflectivity. For the Kramers-Kronig (KK) analysis of the phonon modes (to be described below), we would like to have the reflectivity down to zero photon energy; therefore we complete the experimental spectrum in the following way: With the experimentally determined half-width of the lowest-energy reflectivity peak (assuming it to be symmetric in shape), we construct the low-energy shoulder and determine the

reflectivity at zero photon energy by a self-consistent iterative process in the dielectric functions (discussed below). The finally chosen reflectivity outside the experimental spectrum is shown with a dashed line in the insert of Fig. 1.

In the interband region of the spectrum, we observe a well-structured reflectivity with values between 11% and 18% as typical also for the Eu monochalcogenides.¹⁴ To compute the dielectric functions $\epsilon(\omega)$ with a KK relation, we have to extrapolate the spectrum also to infinite photon energies. This procedure, however, is a standard one and is well described in Ref. 14. Finally, we show in Fig. 2 the real (ϵ_1) and the imaginary (ϵ_2) part of the dielectric function for Eu_3O_4 in the interband region.

IV. INTERBAND TRANSITIONS AND ENERGY-LEVEL SCHEME

It has been an important object of our investigations to derive for the first time the electronic structure of an A_3B_4 compound over a large energy scale. Therefore, an energy-level scheme shall be proposed after identifying electronic transitions in the optical spectra. As it turns out, the well-known electronic structure of EuO (Refs. 13, 14) will be a great help for this purpose, and frequently a comparison will be made.

Starting with low energies in Fig. 2, ϵ_1 steeply increases from negative values, intersects the abscissa at an LO phonon mode, and reaches a plateau at about 1 eV. Since in this energy range ϵ_2 is zero, the plateau defines $\epsilon_{\text{opt}} = 4.15$ and the refractive index $n_{\text{opt}} = 2.05$. A comparison with EuO (ϵ_{opt} between¹⁴ 4.6 and¹⁵ 3.85) yields similar values. On the other hand, the energy gap $E_g = 1.60$ eV is appreciably larger in Eu_3O_4 than in EuO (1.12 eV). Considering a theoretical energy-level diagram based on an ionic model,¹⁶ it becomes

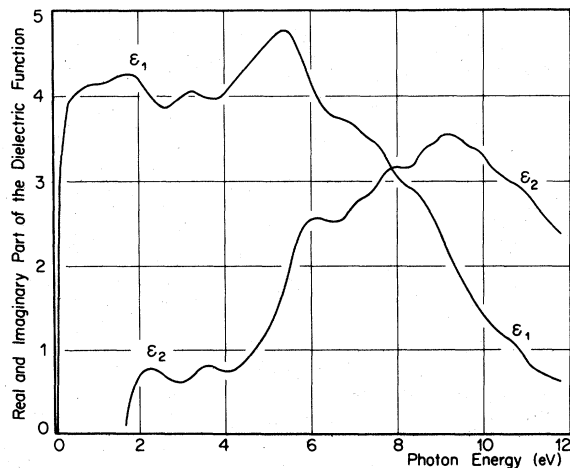


FIG. 2. Real and imaginary part of the dielectric function of Eu_3O_4 .

evident that in Eu_3O_4 as well as in EuO , the localized divalent $\text{Eu } 4f^7$ states are the highest-occupied valence states. But in Eu_3O_4 their density is only $\frac{1}{3}$ the one of EuO . The spectrum of ϵ_2 in Fig. 2 exhibits two maxima at 2.25 and 3.55 eV with about $\frac{1}{3}$ the magnitude observed in EuO , where indeed the two most prominent low-energy peaks have been identified as arising from $4f^7 \rightarrow 4f^6(^7F_J) \times 5dt_{2g}$ and $4f^7 \rightarrow 4f^6(^7F_J)5de_g$ transitions. In Eu_3O_4 the crystal field acting on the $5d$ conduction bands is not cubic; thus a distinction in t_{2g} and e_g should be avoided. Nevertheless, the cubic term will be the largest in a perturbation treatment and effectively the $5d$ conduction band will split in two subbands, their centers being 1.3 eV apart. This value in Eu_3O_4 is much smaller than in EuO (3.1 eV), but as a consequence, just as in the series of the Eu monochalcogenides, a smaller crystal-field-splitting results in a larger energy gap as observed. We thus have strong quantitative and qualitative evidence that the two lowest energy peaks of ϵ_2 in Eu_3O_4 correspond to $4f^7 \rightarrow 4f^6(^7F_J)5d$ transitions into a crystal-field-split $5d$ conduction band. Further evidence is given by the magnetic induced shift of the absorption edge as will be described below.

Once we have chosen the value of $\Delta = 1.3$ eV for the $5d$ crystal-field splitting, it serves as a scale for the further identification of the spectrum. The same value of Δ characterizes the difference between the next two maxima in ϵ_2 at 5.9 and 7.2 eV. From the position in energy, the steep increase in intensity, and from ultraviolet-photoemission (UPS) measurements on EuO ,^{17,18} we conclude that these peaks are due to transitions from the $2p$ valence band of the oxygen ions into the crystal-field-split $5d$ conduction band.

The higher-energy spectrum of ϵ_2 is characterized by a fine structure superimposed on a broad hump. Most probably the latter is due to transitions from the $2p$ valence band into the $6s$ conduction band. So we are left with possible transitions from the Eu^{3+} ions $4f^6(^7F_0)$ into the crystal-field-split $5d$ bands. The key for the identification of this part of the spectrum is the Coulomb correlation energy U between Eu^{2+} and Eu^{3+} ions, and the fact that the final coordination of the $\text{Eu}^{3+}(^7F_0) \rightarrow 5d$ transition must be $4f^5(^6H_J, ^6F_J, ^6P_J)5d$.

The Coulomb correlation energy U is the difference in ionization potentials for the Eu^{2+} and Eu^{3+} energy level. In an energy-level diagram, one always displays, the, e. g., $4f^n$ energy states in a $4f^{n-1} +$ electron configuration, meaning that the energy difference which one reads in the diagram represents the energy which one has to supply to the crystal in order to make this transition.¹⁶ To estimate U from ionization potentials in the case of Eu^{2+} and Eu^{3+} we need the difference be-

tween the third and the fourth ionization energy of Eu . Unfortunately, only the first three ionization energies for Eu are known, the third being 25.13 eV.¹⁹ However, plotting the square root of the sum of the ionization energies versus the number of ionized electrons one obtains a straight line,²⁰ which permits an estimate of the fourth ionization potential of Eu , which is about 31 eV. The difference between the third and the fourth ionization energy for Eu then is about 5.8 eV, which gives us a first estimate of the correlation energy U .

Another theoretical value of U may be obtained by comparing electronic energy levels in rare-earth metals,²¹ where one uses for trivalent Eu metal an interpolation between Sm and Gd metal and for divalent Eu metal the computed values. This procedure yields 5.5 eV for U .

Experimental data for U have been determined from x-ray-photoemission (XPS) measurements, comparing, e. g., the energy levels of EuF_2 containing Eu^{3+} as impurities²² or comparing two different materials, e. g., Eu_2O_3 and EuSO_4 with reference to the carbon $1s$ line of simultaneously present organic contaminants.²³ The experiments yield $U = 6$ and 5.9 eV, respectively.

In our experiment on Eu_3O_4 , we obtain U experimentally by identifying the peak in ϵ_2 at 7.95 eV with the onset of the $4f^6 \rightarrow 5d$ transition and taking the difference to the $4f^7 \rightarrow 5d$ transition: $7.95 \text{ eV} - 2.25 \text{ eV} = 5.7 \text{ eV}$. This value is in good agreement with the theoretical estimates and with the XPS results. It is thus the first time that a Coulomb correlation energy has been determined from an optical reflectivity measurement.

Now we have to consider that in an intracation transition like $4f^6 \rightarrow 5d$, the remaining $4f^5$ electrons can be with a certain probability in excited states allowed by spin conservation and spin-orbit coupling. These are the $4f^5(^6H_J, ^6F_J, ^6P_J)$ multiplets, which are well known from the isoelectronic Sm^{2+} spectra.²⁴ In UPS or XPS electron emission spectra, the probability to find an electron in one of the multiplets can be computed as the "coefficients of fractional parentage"²⁴ because the final state of the emitted electron is a plane wave. In our case of an optical absorption, the final state is a $5d$ conduction band which complicates the situation. Nevertheless, the separation in energy of the multiplets remains the same as in an XPS measurement and it can also be taken from an energy-level scheme of the ions.²⁵ Finally, we have to consider that all these transitions appear twice because of the crystal-field splitting of the $5d$ band.

Helping the reader to select the transitions, we show in Fig. 3 again ϵ_2 of Eu_3O_4 with all the significant energy splittings indicated. This assignment has so many self-consistent checks that no other interpretation is possible. A last remark concerns

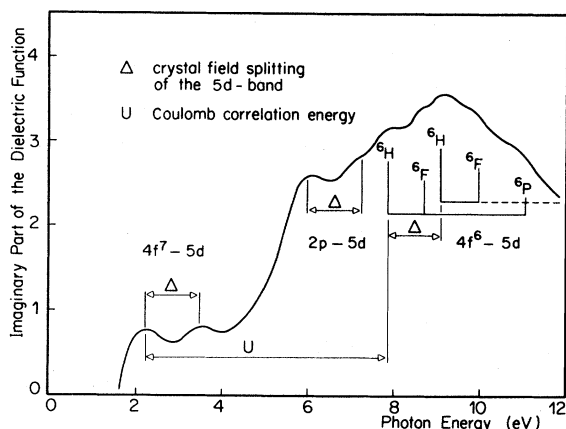


FIG. 3. Imaginary part of the dielectric function. Indicated in the figure is the crystal-field splitting of the $5d$ conduction band and the Coulomb correlation energy. Furthermore, shown is the center of gravity of the 6H , 6F , and 6P multiplets with the intensity computed from the coefficients of fractional parentage.

the only weak contribution to ϵ_2 of the Eu^{3+} transitions in the vacuum ultraviolet spectral region. This can be understood already with classical dispersion theory. Comparing two oscillators with the same oscillator strength but at different resonance frequencies the one at higher energies contributes to ϵ_2 only the fraction ω_1^2/ω_2^2 ($\omega_1 < \omega_2$) of the one at lower energies. This even overcompensates the fact that the Eu^{3+} ions are present twice as much as the Eu^{2+} ions.

From all these data it is now possible to propose a rough energy-level scheme for Eu_3O_4 . For reasons of comparison, we show it in Fig. 4 together with the energy-level scheme of EuO . As reference level we have chosen the $4f^7$ states of divalent Eu.

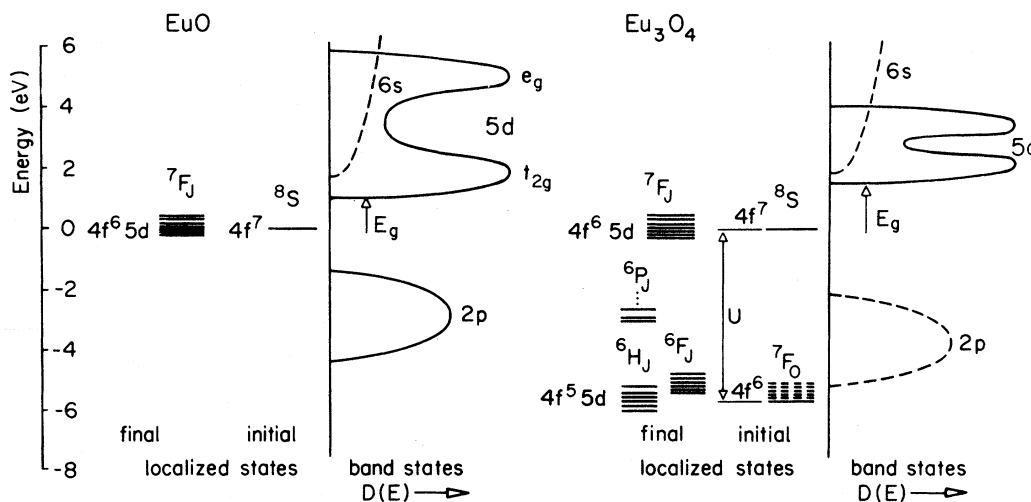


FIG. 4. Energy-level diagram of EuO and Eu_3O_4 . Dashed are shown the excited states ${}^7F_{1\dots 6}$ of the $4f^6({}^7F_0)$ ground state.

On the right-hand side of each diagram we plot the band states, and on the left-hand side, the localized $4f$ states which are furthermore distinguished in initial and final states. The width of the $2p$ valence band is chosen to be the same for both compounds, and it has been taken from photoemission measurements on EuO .^{17,18}

It is obvious that the main differences between both compounds are the existence of the Eu^{3+} $4f^6({}^7F_0)$ level, 5.7 below the Eu^{2+} $4f^7({}^8S_{7/2})$ level of Eu_3O_4 and a reduced crystal-field splitting of the $5d$ conduction band in Eu_3O_4 , resulting in a larger energy gap E_g . It is possible that the width of the $2p$ valence band in Eu_3O_4 is different from the one in EuO , but we do not expect an observable crystal-field splitting since the different oxygen surroundings of divalent and trivalent Eu will wash out any fine structure. Finally, it is not a trivial assumption that the $4f^6 5d$ and $4f^5 5d$ states belong to the same conduction band; however, it seems to be justified by the experiment.

V. PHONON MODES

It has been mentioned above that we expect in Eu_3O_4 two TO and two LO phonon modes due to the different surroundings of Eu^{3+} and Eu^{2+} ions. These modes serve as substitutes for the group theoretically expected many phonon modes. For the KK analysis of the far-infrared spectrum, we had to complete the measured reflectivity (R) to zero frequencies. One procedure has been to construct the low-energy shoulder from the known half-width of the reflectivity curve. A further condition for the reflectivity at zero frequency was that ϵ_2 had to become zero for low frequencies without reaching negative values. An iterative procedure in the dielectric functions gave the results displayed in Fig. 5.

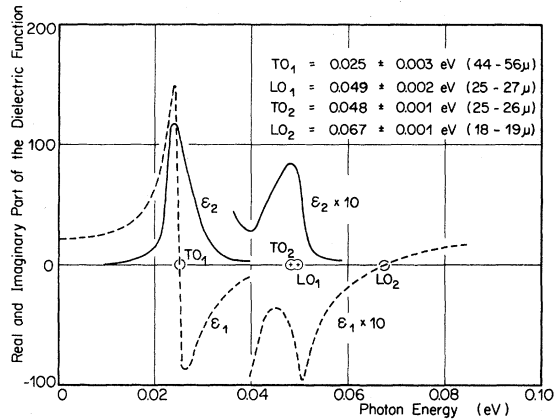


FIG. 5. Real and imaginary part of the dielectric function of Eu_3O_4 in the phonon region. For energies larger than about 0.04 eV ϵ_2 and ϵ_1 are multiplied by a factor 10.

The resonances are given by the zeros of ϵ_1 with $d\epsilon_1/d\omega < 0$ corresponding to a TO mode and $d\epsilon_1/d\omega > 0$ corresponding to a LO mode. The highest-energy LO₂ mode is at $0.067 \pm 0.001 \text{ eV } (18.5 \pm 0.5 \mu\text{m})$, and its position in energy does not depend on the extrapolation procedure of R towards zero frequency. Due to the superposition of the dispersion of the phonon modes, ϵ_1 has only one other zero at the TO₁ mode at $0.025 \pm 0.003 \text{ eV } (50 \pm 6 \mu\text{m})$. This mode depends on the extrapolation procedure of R , but only within the given error limits without inducing further unphysical behavior in ϵ_1 and ϵ_2 . Also, the magnitudes of ϵ_1 and ϵ_2 near the TO₁ mode strongly depend on the extrapolation used, and we give it only a qualitative aspect. The TO₂ mode is best taken from the maximum in ϵ_2 which is at $0.048 \pm 0.001 \text{ eV } (25.5 \pm 0.5 \mu\text{m})$, again it does not depend on the extrapolation of R . The LO₁ mode can be obtained from a decomposition of ϵ_1 and it coincides approximately with the TO₂ mode. The higher-energy TO₂ and LO₂ modes are due to the Eu^{3+} surrounding, and their position in energy is well established. The lower-energy TO₁ and LO₁ modes are due to the Eu^{2+} surrounding and within a larger-error limit also their position in energy can be given.

Finally, the static dielectric constant is shown to be 22 ± 3 , a value which is similar to the one of EuO [23.9 ± 4 (Ref. 12) or 26.5 (Ref. 14)].

VI. OPTICAL TRANSMISSION

Besides the reflectivity of Eu_3O_4 , we also have investigated the optical transmission of thin single crystal plates. In Fig. 6 we display the absorption coefficient K versus the photon energy at 300 K. Between the phonon absorption (residual ray band) below about 0.08 eV and the interband absorption above about 1.6 eV, we observe three groups of sharp absorption lines. Their spectral

position and absorption coefficient clearly identifies them as intra $4f^6$ transitions of trivalent Eu. In Fig. 4 we have indicated the six ${}^7F_{J=1..6}$ multiplet levels with dashed lines. It is, however, remarkable that only transitions are observed from the ground state 7F_0 into states with even J . Besides Eu^{3+} also Pr^{3+} , Tb^{3+} , and Ho^{3+} show electric-dipole transitions only between $J=0$ and even J states.²⁵ Judd²⁶ and Ofelt²⁷ have derived some theories about intensities of optical transitions in crystal-field split $4f^n$ multiplets. In their considerations, they take into account that the wave functions of a given J can have admixtures of opposite parity due to the crystal field and that these admixtures determine the intensity of the electrical-dipole transitions. These authors show indeed that in an ion with an even number of electrons like in Eu^{3+} , transitions from $J=0$ to odd J should be very weak.

In our case the symmetry of the crystal field is so low that the J degeneracy is lifted completely. We thus can have $2J+1$ Stark components. Since the ground state 7F_0 is not split, we only observe the splitting of the final state. Accordingly, we expect in the $J=0 \rightarrow J=2$ transition five absorption lines, in the $J=0 \rightarrow J=4$ transition, nine, and in the $J=0 \rightarrow J=6$ transition 13 absorption lines. As shown in the inserts of Fig. 6, we indeed observe the demanded number of lines with the exception of the $J=0 \rightarrow J=6$ transitions, where even at 2.2 K in a magnetic field of 13.5 kOe, only eight lines can be distinguished. In this case we think that a number of lines overlap or they are not strong enough to be discriminated against the background. In Table I we have compiled the observed intra $4f$ transitions in Eu_3O_4 . We note that there exists also another absorption measurement on Eu_3O_4 ,²⁸ where, however, the absorption coefficient is at least an order of magnitude ($\sim 1000 \text{ cm}^{-1}$) larger

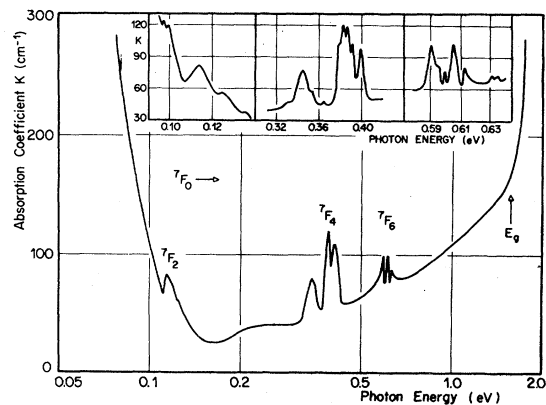


FIG. 6. Absorption coefficient of Eu_3O_4 at 300 K. The fine structure of the ${}^7F_0 \rightarrow {}^7F_2$, 7F_4 , and 7F_6 transitions are shown in the inserts. The one of the ${}^7F_0 \rightarrow {}^7F_6$ transition is shown for 2.2 K in a magnetic field of 13 kOe.

TABLE I. Excitation energy of the 7F_J Stark components above the 7F_0 ground level in eV and μm . (The value in brackets is uncertain.)

7F_2	eV:	0.096	0.102	0.113	0.125	0.134
	μm :	12.9	12.1	11.0	9.90	9.26
7F_4	eV:	0.324	0.343	0.350	0.359	0.380
	μm :	3.83	3.61	3.55	3.45	3.26
		0.383	0.387	0.391	0.397	
		3.24	3.21	3.18	3.13	
7F_6	eV:	(0.568)	0.589	0.593	0.598	0.603
	μm :	(2.18)	2.11	2.09	2.08	2.06
		0.611	0.630	0.635		
	μm :	2.03	1.97	1.95		

than in our samples and the sharp intra $4f^6$ lines are not resolved.

VII. CORRELATION BETWEEN OPTICAL ABSORPTION AND MAGNETIC ORDER

The magnetic properties of Eu_3O_4 have been investigated by several authors.⁷⁻⁹ Holmes and Schieber^{8,9} have found a metamagnetic behavior below $T_N = 5$ K with a critical field $H_c = 2.4$ kOe at 2.2 K. Analyzing their data with a molecular-field theory, they propose the following spin structure: The magnetic moments of the Eu^{2+} ions form linear chains parallel to the c axis of the orthorhombic unit cell. Within these chains, a ferromagnetic alignment exists, while between neighboring chains an antiferromagnetic coupling is present. In these considerations the Eu^{3+} ions do not appear, because at low temperatures only the nonmagnetic 7F_0 ground state is occupied.

We have investigated the position of the absorption edge in the temperature region of magnetic order and also in external magnetic fields up to 13 kOe. The result is shown in Fig. 7. Compared with room temperature, the absorption edge at 10 K is shifted by 0.07 eV towards higher energies. Two competing mechanisms determine the shift of the absorption edge in the paramagnetic region: Upon cooling, a thermal lattice contraction increases the crystal-field splitting of the $5d$ conduction band and as a consequence reduces the energy gap (red shift), and a decreasing electron-phonon interaction narrows the absorbing regions (blue shift). As usual and expected in ionic compounds, the latter effect is larger in magnitude and determines the net result. Between about 40 and 10 K the absorption edge is practically "frozen in."

Cooling near and below T_N , an additional spontaneous blue shift of the absorption edge is observed, which amounts to 0.03 eV until 2.2 K. Extrapolating the indications of a saturation towards zero K, a total blue shift of about 0.035 eV

can be obtained. A blue shift in this order of magnitude is common for antiferromagnets, whereas ferromagnets only exhibit red shifts of the absorption edge. On the other hand, some antiferromagnets are known which also display a red shift of the absorption edge (see compilation below). The decisive factor for this magneto-optic effect is the spin structure of an antiferromagnet which determines sign and magnitude of the local magnetic exchange energy. As illustration, we use two antiferromagnets in zero external fields, with the same crystallographic and electronic structure, namely, EuSe and EuTe . The $4f^7$ spins in consecutive ferromagnetic (111) planes orient in the sequence $\uparrow\uparrow\uparrow\uparrow$ and $\uparrow\uparrow\downarrow\downarrow$, respectively. The total magnetic exchange energy of the $z_1 = 12$ nearest and $z_2 = 6$ next-nearest neighbors is $+6J_1$ for EuSe and $-6|J_2|$ for EuTe . (J_1 is the positive nearest-neighbor exchange, and J_2 is the negative next-nearest-neighbor exchange, and $E = |J_{1,2}| \cos\phi$, with ϕ the angle of the spins with respect to an arbitrarily chosen spin direction, e.g., \uparrow .) The red shift of the antiferromagnetic $\uparrow\uparrow\downarrow\downarrow$ phase of EuSe is thus a consequence of only the positive contributions to the total magnetic exchange energy.

The unusual sharp kink in the blue shift of the absorption edge versus temperature for Eu_3O_4 in Fig. 7 also permits a determination of the Néel temperature in zero fields. It is found to be 5.2

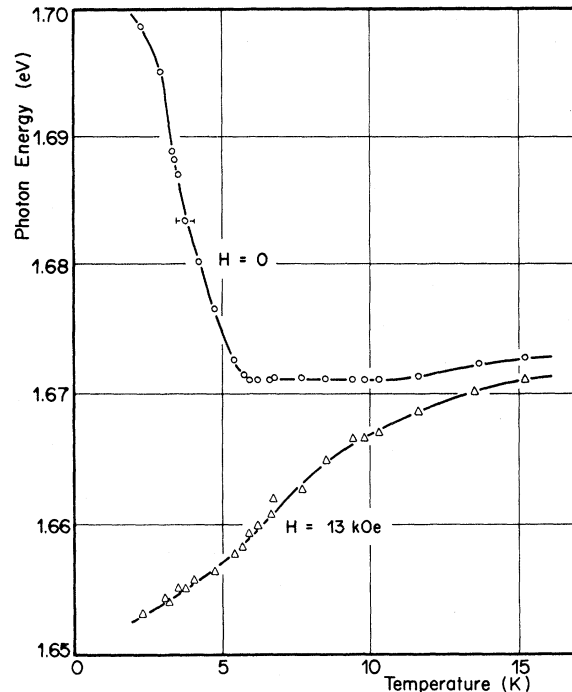


FIG. 7. Position of the absorption edge of Eu_3O_4 vs temperature. $T_N = 5.2$ K.

± 0.2 K, a value which closely agrees with measurements of Holmes and Schieber.^{8,9}

In a magnetic field of 13 kOe perpendicular to the c axis of the crystal, which is in excess of the critical field $H_c = 2.4$ kOe and the anisotropy field of about 7 kOe, a ferromagnetic phase is induced. (Sometimes it is proposed to call such a phase paramagnetic, but we prefer the term "induced ferromagnetism.") As a consequence, we expect and observe a red shift of the absorption edge which amounts to about 0.02 eV between 15 K and zero. At 2.2 K and in function of the magnetic field, the shift of the absorption edge reflects also the kink at the critical field of 2.4 kOe. Thus Eu_3O_4 is the first substance where a blue shift of the absorption edge can be changed into a net red shift.

In this connection it might be of interest to give a more complete inventory of materials on which the shift of the absorption edge has been investigated, because so far, only a very poor compilation has been published.²⁹ The following *ferromagnets* show a red shift: EuO , EuS , EuSe (between 2.8 and 1.8 K),^{30,16} Eu_3P_2 ,³¹ Eu_2SiO_4 ,³² Eu_3SiO_5 ,³³ $\text{EuO}:\text{Gd}$,³⁴ CdCr_2S_4 , CdCr_2Se_4 ,^{35,36} HgCr_2S_4 ,³⁷ HgCr_2Se_4 .³⁸

For the following *antiferromagnets* in zero magnetic field, a red shift (r) or blue shift (b) has been observed: EuSe (between 4.6 and 2.8 K) (r)^{30,39} EuTe (b),⁴⁰ NaCrS_2 (b),⁴¹ ZnCr_2Se_4 (r),³⁵ $\alpha\text{-MnS}$ (b),²⁹ CoO (b),²⁹ MnO (r),^{29,42} Eu_3As_2 (r).³¹

Together with Eu_3O_4 19 materials have been investigated with respect to a shift of the absorption edge.

VIII. CONCLUSION

In this paper we have shown the powerful techniques of optical investigations of semiconductors.

Not only has it been possible to obtain the electronic structure of occupied, localized, and band states, but information is also obtained on the structure and position in energy of empty conduction bands. We have been able to derive the Coulomb correlation energy of Eu_3O_4 by identifying the final $4f^55d$ states. The intra $4f$ transitions further complete the picture of the electronic structure of the material. Also, the basic features of the phonon spectrum have been obtained from the optical investigation. If it were not already known before, we could have derived also the type of magnetic order, the Néel temperature, and the critical field.

The knowledge of the electronic structure of the still relatively simple Eu_3O_4 is of vital importance as a reference of the more complex fluctuating compounds Eu_3S_4 and Sm_3S_4 . The different crystal structure of the latter compounds compared to Eu_3O_4 is not a severe drawback, since it will manifest itself mostly in the magnitude of the $5d$ crystal-field splitting and in the fine structure of the intra $4f$ transitions. Indeed, the optical studies of Eu_3S_4 and Sm_3S_4 have confirmed the statements above.⁴³ The temperature dependence of the optical constants in conjunction with electrical-transport properties will then give information about the hopping mechanism in these compounds. These investigations are under way.

ACKNOWLEDGMENTS

The authors are very grateful to H. P. Staub for technical assistance. The financial support of the Schweizerische Nationalfonds is very much appreciated.

¹U. Buchenau, *Solid State Commun.* **11**, 1287 (1972).

²H. H. Davis, I. Bransky, and N. M. Tallan, *J. Less-Common Metals* **22**, 193 (1970).

³I. A. Smirnov, L. S. Parfen'eva, V. Ya. Khusnutdinova and V. M. Sergeeva, *Fiz. Tverd. Tela* **14**, 2783 (1972) [*Sov. Phys.—Solid State* **14**, 2412 (1972)].

⁴O. Berkooz, M. Malamud, and S. Shtrikman, *Solid State Commun.* **6**, 185 (1968).

⁵F. L. Carter, *J. Solid State Chem.* **5**, 300 (1972).

⁶R. C. Rau, *Acta Crystallogr.* **20**, 716 (1966).

⁷A. A. Samokhvalov, V. G. Bamburov, N. V. Volkenshtein, T. D. Zotov, A. A. Ivakin, Yu. N. Morozov, and M. I. Simonova, *Fiz. Metal Metalloved* **20**, 308 (1965).

⁸L. Holmes and M. Schieber, *J. Appl. Phys.* **37**, 968 (1966).

⁹L. Holmes and M. Schieber, *Phys. Rev.* **167**, 449 (1968).

¹⁰E. Kaldis, in *Crystal Growth, Theory, and Techniques*, edited by C. H. L. Goodman (Plenum, New York, 1974), Vol. I.

¹¹H. Bärnighausen and G. Brauer, *Acta Crystallogr.* **15**, 1059 (1962).

¹²J. D. Axe, *J. Phys. Chem. Solids* **30**, 1403 (1969).

¹³G. Güntherodt and P. Wachter, *Solid State Commun.* **12**, 897 (1973).

¹⁴G. Güntherodt, *Phys. Cond. Matter* **18**, 37 (1974).

¹⁵P. Wachter, *Phys. Kondens. Materie* **8**, 80 (1968).

¹⁶P. Wachter, *CRC Crit. Rev. Solid State Sci.* **3**, 189 (1972).

¹⁷D. E. Eastman, F. Holtzberg, and S. Methfessel, *Phys. Rev. Lett.* **23**, 226 (1969).

¹⁸P. Cotti and P. Munz, *Phys. Cond. Matter* **17**, 307 (1974).

¹⁹L. R. Morss, *J. Phys. Chem.* **75**, 392 (1971).

²⁰R. T. Sanderson, *Chemical Periodicity* (Reinhold, New York, 1963).

²¹J. F. Herbst, D. N. Lowy, and R. E. Watson, *Phys. Rev. B* **6**, 1913 (1972).

²²S. Hüfner and G. K. Wertheim, *Phys. Rev. B* **7**, 5086 (1973).

²³C. K. Jorgensen, *Chimia* **27**, 203 (1973).

²⁴M. Campagna, E. Bucher, G. K. Wertheim, L. D. Longinotti, *Proceedings of the Eleventh Rare Earth Research Conference Traverse City, 1974* (unpublished), Vol. 1, p. 53; P. A. Cox, Y. Baer, and C. K. Jorgensen, *Chem. Phys. Lett.* **22**, 433 (1973).

- ²⁵G. H. Dieke, *Spectra and Energy Levels of Rare Earth Ions in Crystals* (Interscience, New York, 1968).
- ²⁶B. R. Judd, *Phys. Rev.* **127**, 750 (1962).
- ²⁷G. S. Ofelt, *J. Chem. Phys.* **37**, 511 (1962).
- ²⁸M. W. Shafer, J. B. Torrance, and T. Penney, *J. Phys. Chem. Solids* **33**, 2251 (1972).
- ²⁹H-h. Chou and H. Y. Fan, *Phys. Rev. B* **10**, 901 (1974).
- ³⁰G. Busch and P. Wachter, *Phys. Kondens. Materie* **5**, 232 (1966).
- ³¹P. Wachter and J. Wulfschleger, *J. Phys. Chem. Solids* **33**, 939 (1972).
- ³²E. Kaldis, P. Streit, and P. Wachter, *J. Phys. Chem. Solids* **32**, 159 (1971).
- ³³E. Kaldis, P. Streit, S. Vaccani, and P. Wachter, *J. Phys. Chem. Solids* **35**, 231 (1974).
- ³⁴J. Schoenes and P. Wachter, *Phys. Rev. B* **9**, 3097 (1974).
- ³⁵G. Busch, B. Magyar, and P. Wachter, *Phys. Lett.* **23**, 438 (1966).
- ³⁶G. Harbeke and H. Pinch, *Phys. Rev. Lett.* **17**, 1090 (1966).
- ³⁷G. Harbeke, S. B. Berger, and F. P. Emmenegger, *Solid State Commun.* **6**, 533 (1968).
- ³⁸H. W. Lehmann and F. P. Emmenegger, *Solid State Commun.* **7**, 965 (1969).
- ³⁹B. E. Argyle, J. C. Suits, and M. J. Freiser, *Phys. Rev. Lett.* **15**, 822 (1965).
- ⁴⁰P. Wachter and P. Weber, *Solid State Commun.* **8**, 1133 (1970).
- ⁴¹K. W. Blazey and H. Rohrer, *Phys. Rev.* **185**, 712 (1969).
- ⁴²The results were interpreted as due to excitation of localized electrons rather than to the excitation of electrons to the conduction band, as in EuTe.
- ⁴³B. Batogg, E. Kaldis, A. Schlegel, and P. Wachter (unpublished).